Phase Separation in Lipid Bilayers Containing Integral Proteins. Computer Simulation Studies†

Turab Lookman, David A. Pink,* Ernst W. Grundke, Martin J. Zuckermann, and Frances deVerteuil

ABSTRACT: We have constructed a lattice model of a dipalmitoylphosphatidylcholine bilayer containing integral proteins and studied its behavior as a function of temperature and protein concentration, c, by using computer simulation methods. Each site of a triangular lattice can be occupied by a lipid chain in any of ten conformational states which were simplified to two such states, a low-energy temperature-dependent extended chain state and a high-energy melted chain state, by a time-scale argument, in order to facilitate the simulation. The dynamical change of state was modeled by using the Monte Carlo simulation procedure of Metropolis. A hexagon of 19 such sites represented a trans-bilayer protein of molecular weight ~15000. The proteins could occupy cells, which themselves form a triangular lattice superimposed upon the lipid lattice, and could move from one cell to another depending upon whether the other cell was occupied by another protein and, if not, whether the lipids in the other cell and between the two cells were sufficiently melted. This model thus describes both lipid hydrocarbon chain melting and protein lateral motion, but rotational motion was ignored. The free parameter, $K(G)$, describing the interaction between a protein and an adjacent lipid chain in the low-energy state, was determined by fitting the calculated c dependence of ^2H nuclear magnetic resonance (NMR) chain order parameters in the fluid phase to the values measured. Other parameters were taken over from previous calculations, and direct protein–protein interactions were ignored. We calculated the (normalized) number of protein–protein nearest-neighbor pairs, n_{pp}, and found that for $T > T_c$ it was small with large fluctuations, indicating a homogeneous protein lateral distribution with small local protein clusters forming and breaking up rapidly. As T decreased slowly through T_c, n_{pp} increased, and the fluctuations died out at a temperature $T_K < T_c$, indicating the formation of large stable protein clusters. A phase diagram was deduced, and the following three points emerged: Above T_c, there is essentially a single homogeneous phase [unless $K(G)$ is large]. For $T_K < T < T_c$, the system separates into an essentially pure lipid phase and a protein-rich phase containing melted lipids unless $K(G)$ is very large. At T_K, the protein-rich cluster freezes; i.e., the short-time fluctuations in its size cease, and the minimum number of chains are "trapped" inside the cluster. These chains generally remain melted down to a lower temperature. Upon being heated through T_K, the protein cluster starts to come apart (i.e., melt) by melting the lipids on its periphery. We calculated the proportion of lipids giving rise to a 4.2-Å X-ray reflection characteristic of a "crystalline" lipid phase, and the results explain the observations made. Our calculated transition enthalpies are in accord with recent measurements, and we explain how either a linear dependence upon c or a concave curve can come about. We predict that ^2H NMR will detect two populations of lipids for a range of temperatures $T < T_c$: gel-phase lipids in the pure lipid phase and fluid-like lipids in the protein-rich clusters. The latter lipids freeze noncooperatively at temperatures below T_K. For $T_K < T \lesssim T_c$, a complex spectrum might be seen because of exchange between the two phases.

It continues to be of great interest to study the thermodynamic behavior of lipid bilayers reconstituted with integral proteins, as a function of temperature and protein concentration. The reason for this is that observation of quantities such as heats of transition, lateral phase separation, and the statics and dynamics of lipid molecules by using the variety of spectroscopic techniques now available tells us much about lipid–protein and protein–protein interactions. Such information can be of use in understanding the properties of biological membranes. In recent years, a great deal of data has been obtained on a variety of integral proteins incorporated into phosphatidylcholine bilayers, and the intention of this paper is to provide an understanding of some of them within the framework of a relatively simple model. Studies using freeze–fracture electron microscopy and differential scanning calorimetry (Boggs et al., 1980; Gomez-Fernandez et al., 1980), X-ray wide-angle scattering (Hoffmann et al., 1980), and ^2H nuclear magnetic resonance (NMR)[1] spectroscopy (Seelig & Seelig, 1978; Oldfield et al., 1978; Jacobs & Oldfield, 1981) have provided information about the static distribution of certain integral proteins as well as the static order parameters and correlation times of lipid hydrocarbon chain motion. Similar information has been obtained from studies on *Escherichia coli* [see, e.g., Overath & Thilo (1978) and Nichol et al. (1980)] and *Acholeplasma laidlawii* (Smith et al., 1979; Pink & Zuckermann, 1980). Here we shall construct a model of integral proteins which are allowed to diffuse laterally in the plane of a dipalmitoylphosphatidylcholine (DPPC) bilayer membrane. The lipid molecules making up the bilayer are allowed to be in a number of internal states which correspond to various hydrocarbon chain conformations. Using the Monte Carlo techniques of Metropolis (Metropolis et al., 1953; Binder, 1979), we shall study lipid hydrocarbon chain melting. The movement of proteins will be studied by using a simple molecular dynamics method, and equilibrium distributions of proteins within the plane of the membrane will be studied. We shall deduce a phase diagram and study some

† From the Theoretical Physics Institute, St. Francis Xavier University, Antigonish, Nova Scotia, Canada B2G 1C0 (T.L., D.A.P., and E.W.G.), and the Department of Physics, McGill University, Montreal, Quebec, Canada H3A 2T8 (F.deV. and M.J.Z.). *Received April 23, 1982.* This work was supported in part by the Natural Sciences and Engineering Research Council of Canada.

[1] Abbreviations: NMR, nuclear magnetic resonance; PC, phosphatidylcholine; DPPC, dipalmitoylphosphatidylcholine; DSC, differential scanning calorimetry; DMPC, dimyristoylphosphatidylcholine.

0006-2960/82/0421-5593$01.25/0

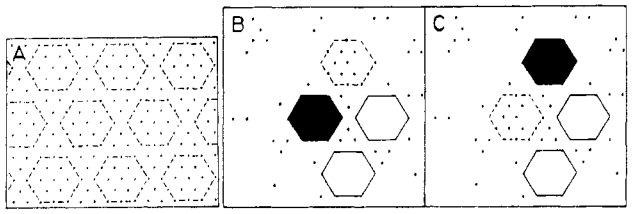

FIGURE 1: (A) Triangular lattice of lipid chain sites (dots) representing the plane of the bilayer and triangular lattice of protein cells (outlined with dashes). Each protein molecule occupies one cell containing 19 lipid chain sites in each half of the bilayer. (B and C) Model of protein motion in the plane of the bilayer. (B) Three cells are occupied. (C) The black protein moves to the dashed cell, the lipid chains within it and the region between the two cells being sufficiently melted. The lipid states in the dashed cell move to the cell vacated by the black protein.

of the measurements referred to above, showing that they can be understood within the framework of this simple model.

Another simulation of proteins in lipid bilayers has been performed (Freire & Snyder, 1982). This simulation differs from ours in the following ways: It does not allow the lipid chains to change their state dynamically as our simulations do, and it does not permit the proteins to move within the plane of the bilayer. Freire and Snyder used the method of Alexandrowicz (1971a,b) to add proteins successively to a bilayer in accord with certain nearest-neighbor interactions between the proteins, and they found that critical cluster formation depended upon the strength of this interaction. The model used by us includes indirect protein–protein interactions, via the lipids, which can change their states dynamically, as well as the provision for direct protein–protein interactions. Because it is not possible to deduce the indirect, lipid-mediated protein–protein interaction in our many-body system, we are not able to compare our results directly with those of Freire and Snyder.

Although it is of interest to study the dependence of the phase diagrams obtained here upon the size of the proteins, we have not undertaken it. The work presented here is intended to show that with protein–lipid interactions deduced from one kind of measurement (^{2}H NMR), the results of many other measurements (DSC, freeze–fracture electron microscopy, and X-ray scattering) can be understood. To extend it to study how proteins of different sizes would modify these general conclusions is beyond the intention of this paper, though we plan to treat this in a study comparing polypeptides and large proteins. We will also ignore any changes in the internal state of the protein.

Theory

Model. We considered a triangular lattice of lipid sites, referred to as the lipid lattice, of 1600 sites with periodic boundary conditions. A protein lattice of 64 protein cells was superimposed upon the lipid lattice such that each protein cell consisted of 19 lipid sites forming a hexagon and represented that part of an integral protein penetrating half of the lipid bilayer (Figure 1A). The protein centers coincided with lipid lattice sites. The proteins could only move from cell to cell on the protein lattice. Each lipid site that was not part of a protein cell was considered to be occupied by a lipid hydrocarbon chain. Likewise, when a protein cell was unoccupied, each lipid site forming the protein cell was considered to be occupied by a lipid hydrocarbon chain. We have assumed that at closest packing the proteins can have some lipids between them but that they are not each surrounded by an unbroken annulus of lipids. Since this paper does not deal with the question of the lipid:protein ratio in protein-rich phases, then this model is acceptable. We have, however, made use of a model such as this to study ^{2}H NMR order parameters in the fluid phase (Pink et al., 1981a) and find that protein close-packing as assumed here is in accord with experiments.

To model the dynamics, we adapted a model used to study Raman scattering by bilayers of phosphatidylcholines (Pink et al., 1980). The Hamiltonian for this system of lipids and proteins is

$$H = -\frac{J_0}{2}\sum_{\langle ij\rangle}\sum_{nm}J(n,m)L_{in}L_{jm} + \sum_{i}\sum_{n}(\Pi A_n + E_n)L_{in} - J_0\sum_{\langle il\rangle}\sum_{n}K(n)L_{in}P_l \quad (1)$$

It is a sum of the terms describing the interaction between two nearest-neighbor lipid chains (first term), the internal energy of a single lipid chain (second term), and the energy of the interaction between a lipid chain which is adjacent to a protein (third term). Each chain can be in one of nine low-energy states, g, 2, ..., and 9, which dominate in a pure lipid bilayer sufficiently far below the main transition temperature, T_c, and one effective high-energy "melted" state, e, which dominates above T_c. L_{in} is a projection operator for site i when a chain is in state n; $J(n,m)$ is the van der Waals interaction energy between adjacent chains in states n and m. A_n and E_n are the area and internal energy, respectively, of a chain in state n, and Π is an effective lateral pressure. The effect of repulsive steric interactions has been taken into account by the choice of the conformations that go to make up the nine low-lying states, and the static ^{2}H NMR order parameter plateau arises even when $J_0 = 0$ (Dill & Flory, 1980). The states were described by Pink et al. (1980), where their properties were listed. However, for convenience of performing the Monte Carlo simulation, we shall simplify the system to a two-state model by using the following time-scale argument. The time scale for transitions among the lowest lying states is of the order of 10^{-10}–10^{-11} s, while that between the low-lying states and the highly excited melted state e is of the order of 10^{-6} s (Skolnick & Helfand, 1980; Weber, 1978; D. A. Pink, unpublished results). In the main lipid bilayer phase transition, one is concerned with processes taking place on the latter time scale; hence, a thermal average over the nine low-lying states may be performed to obtain an effective ground state, G. Care must be taken in performing this average because the low-lying states interact with each other, and the interaction energies are not all the same. However, because there are no phase transitions taking place within the nine low-lying states, the interactions between these states may be represented by mean fields in performing the thermal average over the nine states to obtain an effective temperature-dependent ground state G (Georgallas & Pink, 1982; Pink et al., 1982). Accordingly, the state labels n and m of eq 1 range over only G and e, and the site labels i and j are restricted to be nearest neighbors; i.e., only nearest-neighbor lipid hydrocarbon chains interact via the van der Waals interaction with each other. P_l is a protein projection operator for protein cell l. K(G) and K(e) describe the interaction energies between a protein and a lipid chain in the G or e state adjacent to it. ^{2}H NMR measurements on a variety of integral proteins (Kang et al., 1979; Rice et al., 1979) can be interpreted as showing that they all interact only weakly with PC chains in excited states. Accordingly, we chose K(e) = 0. As a first approximation, the protein–protein interactions will be taken to be zero, although this is an important point which will be taken up elsewhere.

Simulation Methods. We are interested in discovering if and how phase separation takes place in the lipid–protein bilayer. We shall adopt the picture that the proteins diffuse

in the plane of the bilayer, easily when the lipid chains adjacent to them are sufficiently statically disordered and with difficultly otherwise. The diffusion of the lipid chains will be ignored, as a first approximation, and we shall thus be concerned with modeling the following two dynamical changes: the lipid hydrocarbon chain change of state via trans–gauche isomerization and the lateral diffusion of the proteins. We shall model the first process as a Monte Carlo simulation, while the protein motion will be modeled as a Markov process in which proteins move preferentially in directions in which the lipid hydrocarbon chains display a sufficient amount of static disorder. The second process is thus not a Monte Carlo simulation. The two processes are described in detail below.

(*A*) *Protein Motion Simulation.* As the criterion for protein lateral diffusion to occur, we adopted the following condition: A protein can move from one protein cell to a nearest-neighbor protein cell if the second cell is unoccupied by another protein and if all the lipids occupying that cell as well as the intervening region between the cells are sufficiently melted (Figure 1B,C). We shall refer to the area comprising the second protein cell and the intervening region between it and the first protein cell as a sector associated with the first cell. The lipids in a sector were considered to be sufficiently melted if they had a probability averaged over one Monte Carlo "step" (see below for its definition), greater than or equal to a preset value, p, of being in the melted state e. This method of protein movement from one cell to a neighboring cell represents not a continuous monitoring of protein motion but a sequence of "snapshots" taken over the time scale characteristic of a protein moving through a distance equal to its diameter. This is the time scale of our study of lateral phase separation. We consider that it is unnecessary to concern ourselves with the details of the mechanism of protein lateral diffusion in a lipid bilayer. Furthermore, because the only lateral diffusion in which we are interested is that of the proteins, we shall keep the chains fixed at their lattice sites unless they are displaced by proteins as described below. A protein was visited randomly and one of the six possible directions in which it could move was randomly chosen for it to move in. If the nearest-neighbor cell in the chosen direction was occupied by another protein, or if the lipids within the sector in question were not sufficiently melted, the protein was not allowed to move. If the nearest-neighbor protein cell in the chosen direction was unoccupied and the lipids within the sector were sufficiently melted, the protein was allowed to move to the neighboring cell, and the displaced lipids were placed in the vacated protein cell. Each lipid displaced from a position in the protein cell occupied the corresponding position in the vacated protein cell. The mechanism by which the lipids were displaced due to the protein movement was not considered crucial since the system was allowed to equilibrate between the protein motion from cell to cell.

(*B*) *Monte Carlo Simulation of Lipid Chain Change of State.* The lipid hydrocarbon chain change of state was carried out by using the method of Metropolis (Metropolis et al., 1953; Binder, 1979). Each Monte Carlo "pass" consisted of randomly visiting each of the lipid chains only once and deciding whether or not the chains would change their state (i.e., G to e or e to G). At each site occupied by a chain, the local energy, that is, the energy associated with the configuration consisting of the site in question ("central site") and its six nearest neighbors, was considered, and if this could be lowered by a change of state of the lipid chain at the central site, then the change was made. However, if the local energy would be increased by the change of state of this chain, then the state of the lipid chain was changed only if the quantity $\exp[-(\text{energy change})/(k_B T)]$ was greater than a randomly generated number between 0 and 1. Here, k_B is Boltzmann's constant and T the absolute temperature. Each Monte Carlo step consisted of two Monte Carlo lipid passes followed by a visit to each of the proteins in a random order to decide if they would move or not. We found two lipid passes sufficient to allow the lipids to approximately equilibrate between protein motion. Thus, each Monte Carlo step is equivalent to an effective elapsed time for attempted protein movement so that the sequence of Monte Carlo steps can be interpreted as the progression of time. At the end of each Monte Carlo step, bulk thermodynamic averages for that state in the ensemble were evaluated. We studied the enthalpy, Q, the number of pairs of nearest-neighbor proteins, $n_{pp}(T)$, and the average number of lipid chains in the states G and e as functions of the temperature T, the protein concentration, the value of $K(G)$, and the number of Monte Carlo steps. The random order of visiting each lipid site and each protein was regenerated for each pass and step by a "shuffling" algorithm in order to obtain a representative sample of phase space. This method has been tested on calculations involving the two-dimensional Ising model, for which exact results are known, and no suggestion of restricted phase space sampling has emerged. The random number generator used here (RANF on a CDC Cyber 170-720) suffers from the usual defects of all random number generators that we know of [e.g., see Marsaglia (1968)]. These had, apparently, no adverse effect upon our sampling. Some of the simulations reported here were also performed, for purposes of checking the programs, upon an HP3000 series 3 machine by using our own random number generator, and we found that differences in, for example, the average area per lipid chain were less than $\sim 1\%$. All quantities that we calculated converged very rapidly (within 10^2 steps). The lipid chain quantities converged much more rapidly than this, and the reason is that the chain melting model is equivalent (isomorphic) to the two-dimensional Ising model *in the presence of a magnetic field* (Georgallas & Pink, 1982). Here, the system is sufficiently far from its critical point such that the correlation lengths are small (less than or equal to a few lipid lattice constants), and no critical fluctuations really develop. Comments upon the rapidity of convergence in this model have been made by Georgallas & Pink (1982).

In some of the cases discussed here, various different initial protein distributions and total number of passes for each temperature were used, but the results were all essentially the same. For example, the average cyclomatic index (see below) varied by $\lesssim 4\%$, a value reflecting the small number of proteins used. The initial state of the lipid chains was always taken to be that in which each chain was in its G state, but, as mentioned above, we have always found results in accord with cases in which exact results are known (Georgallas & Pink, 1982).

Choice of $K(G)$. We have performed a mean field approximation (D. A. Pink et al., unpublished results) on a Hamiltonian having the form of eq 1 and have found that values of $K(e) = 0$ and $K(G) = 0.34$ for each lipid chain adjacent to a protein will reproduce the dependence of the ^2H NMR order parameters upon protein concentration in a fluid phase of DMPC bilayers (Kang et al., 1979; Rice et al., 1979). In the Monte Carlo simulation, each lipid chain site interacts with six nearest-neighbor sites. For the case of an isolated protein, there are 18 chain sites adjacent to it. Six of these interact with five other lipid sites and one site belonging to

a protein, while twelve of them interact with four other lipid sites and two sites belonging to the protein. Since our simulation involves keeping a record of the states of the six nearest neighbors to every lipid chain, it can be seen that we may not assign a value of $K(G) = 0.34$ to every bond connecting a chain with a protein site. Instead, we chose a value such that $K(G)$ averaged over all sites around a protein yielded a value of 0.34. This gave $30K(G) = 0.34 \times 18$, which gave $K(G) = 0.204$. No such difficulties occur for $K(e)$ which was simply chosen to be zero. We also studied the system for the case that $K(G) = 0.40$. This converts to a lipid–protein interaction of 0.667 when the lipid is in the G state. An interaction of this strength corresponds more to the case of cholesterol (Pink et al., 1981b) than to a protein.

Results

For a value of p, which determined whether the lipid chains in a sector were sufficiently melted in order that a protein could move to the cell in question, we chose $p = 0.5$. This value allowed a sufficiently rapid movement of proteins so that convergence of the protein dynamical variables had occurred by $\sim 10^2$ Monte Carlo steps, for the cases which we studied, but was sufficiently high so that the diffusion coefficient of a single isolated protein decreased markedly as the temperature was decreased through T_c. The second condition is a necessary condition upon p, but we did not study what range p could have in accord with this restriction.

We were interested in studying thermodynamic functions such as the transition enthalpy, Q, and the probabilities of lipid chains being in their ground or excited states, $\langle N_G \rangle$ and $\langle N_e \rangle$, as functions of temperature and protein concentration. We were also interested in studying protein clustering, and to this end, we calculated $n_{pp}(T)$, the number of proteins which were nearest neighbors on the protein lattice for each Monte Carlo step as well as the average over all steps at a given temperature. From the definition of cyclomatic index, we have

$$n_{pp}(T) = C(T) + N_p - k \qquad (2)$$

where $C(T)$ is the cyclomatic index (Domb & Stoll, 1977; Stoll & Domb, 1979), N_p the number of proteins for the concentration c, and k is the number of components. $n_{pp}(T)$ represents the degree of clustering, with a large value denoting compact clusters and a small value denoting a distribution in which clusters may appear to be absent. We normalized $n_{pp}(T)$ with respect to the maximum possible number of protein–protein nearest neighbors at that concentration so that $0 \leq n_{pp}(T) \leq 1$.

We studied the effect of integral proteins upon a model of bilayer of DPPC. With $J_0 = 0.7428 \times 10^{-13}$ erg, the main lipid transition temperature was adjusted to be $T_c = 41$ °C, and no provision was made in the model for any other pure lipid phase change such as the pre- or subtransitions since these vanish for the protein concentrations in which we are interested. As stated before, we used a lattice of 1600 lipid sites and 64 protein cells. This corresponds to a bilayer-spanning protein of molecular weight ~15 000. With each protein penetrating both sides of the bilayer, 10 proteins corresponds to a lipid:protein ratio of 141:1 while 20 such proteins correspond to a ratio of 61:1.

Figure 2 shows results for $n_{pp}(T)$ as a function of protein concentration when the system was cooled slowly. Here, the system was brought to equilibrium for 20 Monte Carlo steps at 44 °C and then allowed to remain at that temperature for 250 such steps. The value of $n_{pp}(T)$ was recorded every 25 Monte Carlo steps while its average value, $\overline{n_{pp}(T)}$, for that

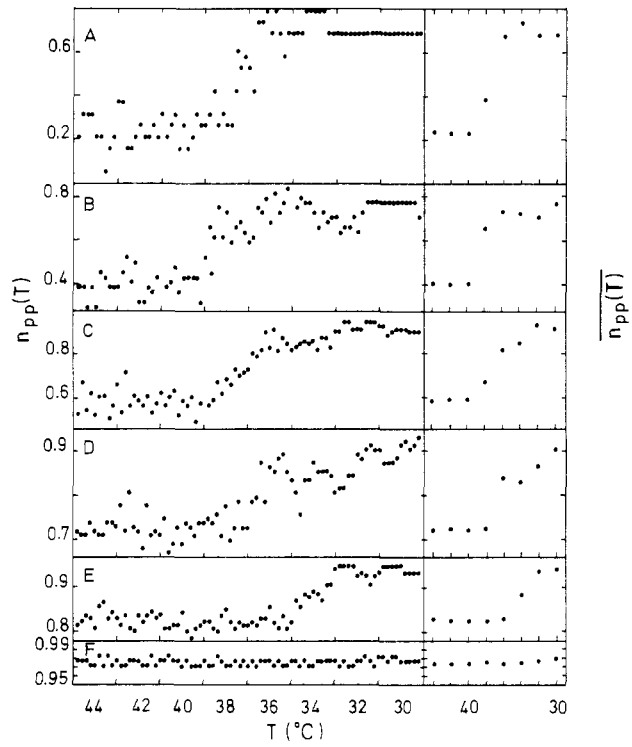

FIGURE 2: Number of protein–protein nearest neighbors, $n_{pp}(T)$ (left panels) and $\overline{n_{pp}(T)}$ (right panels), for $K(G) = 0.204$ and various protein concentrations, under conditions of slow cooling (see text) in a DPPC bilayer. For $n_{pp}(T)$, each point represents its instantaneous value every 25 Monte Carlo steps, with the temperature being reduced by 2 °C every 250 steps. The system was first brought to equilibrium at 44 °C before being cooled. For $\overline{n_{pp}(T)}$, the points represent the average value of $n_{pp}(T)$ over 250 steps for each temperature. The number of proteins is the following: (A) 10; (B) 20; (C) 30; (D) 40; (E) 50; (F) 60. Fluctuations in $n_{pp}(T)$ indicate fluctuations in protein clustering.

temperature was calculated over all 250 such steps. At the end of the 250 steps, the temperature was reduced by 2 °C and the system equilibrated for 20 steps. A further 250 steps were then performed with instantaneous values of $n_{pp}(T)$ being recorded as before, and at the end, the average value $\overline{n_{pp}(T)}$ was calculated. This procedure was repeated until a temperature range from 44 to 30 °C had been covered. The sets of points for each concentration in Figure 2 can be divided into three regions (with the possible exception of Figure 2F, for 60 proteins). The first region is from high temperatures (here 44 °C) to some lower temperature, e.g., ~40 °C in the case of 20 proteins, in which the lipids are all essentially melted. There we see large fluctuations in $n_{pp}(T)$ superimposed upon a relatively small constant value of $\overline{n_{pp}(T)}$. In this region, the protein distribution might appear to be "random". Small protein clusters form locally but quickly break up and re-form elsewhere. The second temperature region is that in which $n_{pp}(T)$ rises as T is decreased though the fluctuations persist. For the case of 20 proteins, this is from ~40 to ~32 °C. Here the lipids are starting to freeze, and because the proteins move only in sufficient melted regions, they move toward each other where possible. However, because the disordering effect of the proteins is still "experienced" by the lipids, there are areas of lipids associated with the proteins which can fluctuate between the G and e states, so that the value of $n_{pp}(T)$ fluctuates. Thus, the protein "clusters" are not static but are dynamically fluctuating as time goes by. Finally, in the third region, below ~32 °C, those lipids not sufficiently close to the proteins have effectively frozen into their G states and in doing so freeze

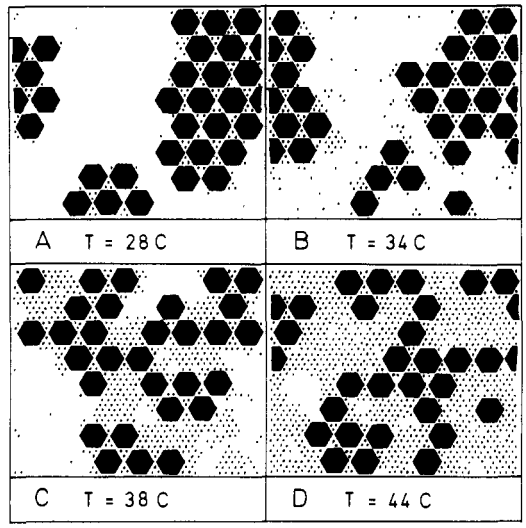

FIGURE 3: Typical protein distributions for $K(G) = 0.204$ [with the value of $n_{pp}(T)$ near its average] at various temperatures for 30 proteins ($c = 0.028$). Black hexagons represent proteins, dots represent lipid chains in their e (melted) states, and blank areas represent lipid chains in their G (extended) states. (A) Phase separation into a protein-rich and a pure lipid phase at $T = 28$ °C $< T_K$ ($\approx$32 °C here). (B) The protein-rich "patch" starts to melt by melting lipid chains on its periphery so that the proteins begin to diffuse apart at $T = 34$ °C $> T_K$. (C) The protein patch melting has progressed further at $T = 38$ °C. (D) The remainder of the lipid chains melt at $T \approx T_c = 41$ °C, and the bilayer is made up of mostly melted chains and diffusing proteins, which will appear homogeneously distributed for a sufficiently large system, at $T = 44$ °C. Note the fluctuations in the lipid chain states which will influence trans-bilayer diffusion (Zuckermann & Pink, 1980).

out the fluctuations in protein clusters. The clusters are now static and essentially remain so as the system is cooled further. It can be seen that the change in $\overline{n_{pp}(T)}$ as well as the amplitude of the fluctuations decreases as the protein concentration increases. This is because at high concentrations close protein packing implies a relatively high value of $\overline{n_{pp}(T)}$ and small fluctuations.

This description is completely reversible, though there might be "hysteresis-like" behavior if too rapid heating and cooling rates are used, and four instantaneous distributions are shown in Figure 3 for the case of 30 proteins. A distribution achieved at 28 °C is shown in Figure 3A. The system, on being cooled as described above, phase separated into the protein-rich region (the protein-rich areas actually comprise a single cluster because of periodic boundary conditions) and a pure lipid phase. It can be seen that most of the lipid chains inside the cluster are in the excited, e, state; i.e., they are statically disordered. This is a consequence of the protein–lipid interaction, $K(G)$, deduced from ^2H NMR measurements performed in the fluid phase of lipid–protein bilayers. As the temperature is raised above a temperature T_K, $T_K \approx 32$ °C in the case considered here, the protein clusters begin to "melt". This is manifested by the formerly frozen lipids close to the periphery of the protein clusters melting and allowing the protein clusters to "come apart" (Figure 3B). As the temperature is raised higher, the clusters come apart more, as more lipids are melted (Figure 3C). At some temperature in the neighborhood of T_c (in this case of 30 proteins, $\sim$39 °C), the remaining unmelted lipids melt, and the proteins display a "random" distribution since they are now free to diffuse in any direction not blocked by other proteins (Figure 3D).

We are now in a position to deduce an approximate phase diagram for this system. From Figure 2, if, as the temperature is increased, we let the onset of "protein cluster melting"

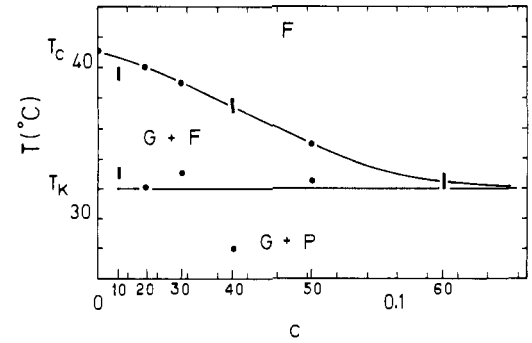

FIGURE 4: Approximate phase diagram for a DPPC–protein ($M_r \simeq 15000$) bilayer with $K(G) = 0.204$, deduced from Figure 2 as described in the text. F denotes a fluid phase of homogeneously distributed proteins in a bilayer of predominantly melted lipids (Figure 3D). G denotes an ordered essentially pure lipid phase with the chains extended (e.g., the blank areas of Figure 3A), and P denotes the protein-rich phase (the protein cluster of Figure 3A). The number of proteins is related to their concentration as shown. $T_c = 41$ °C is the main melting temperature of a bilayer of pure DPPC, while T_K ($\approx$32 °C) is the temperature at which the protein-rich "cluster" begins to melt. The replacement of dots by vertical lines, at 10, 40, and 60 proteins, indicates uncertainty in the temperature of the process in question.

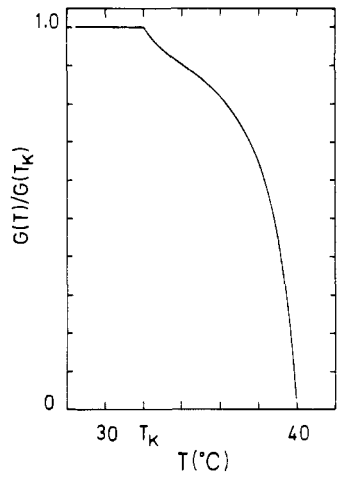

FIGURE 5: Amount of ordered lipid phase existing at $T > T_K$ [$G(T)$ compared to the amount $G(T_K)$, at T_K], calculated from the phase diagram of Figure 4 for 20 proteins. This quantity should be directly proportional to the intensity of the 4.2-Å reflection in wide-angle X-ray scattering [compare Figure 5 of Hoffmann et al. (1980)].

indicate one phase boundary, and the end of lipid melting indicate a second one, then we obtain the phase diagram shown in Figure 4. The two changes are indicated for each protein concentration, and the phase boundaries are drawn approximately through these points. They are necessarily approximate, and we are unable yet to say whether the boundaries extend to $c = 0$. The reason for the anomalously low temperature for the onset of "cluster melting" in the case of 40 proteins is not clear, but we hesitate to deduce a more complicated phase diagram than the one drawn from such little information.

We see that for $T < T_K \approx 32$ °C in this case, the system separates into essentially pure lipid and protein-rich phases. If we assume that the pure lipid phase will crystallize into a triangular lattice and so give rise to a 4.2-Å reflection in wide-angle X-ray scattering, while the lipids in the protein-rich phase, being melted, will make no contribution to this reflection, then we can calculate the intensity of this reflection as a function of temperature. Figure 5 shows the calculated intensity of the 4.2-Å reflection, for the case of 20 proteins, as a function of temperature. The intensity is constant up to

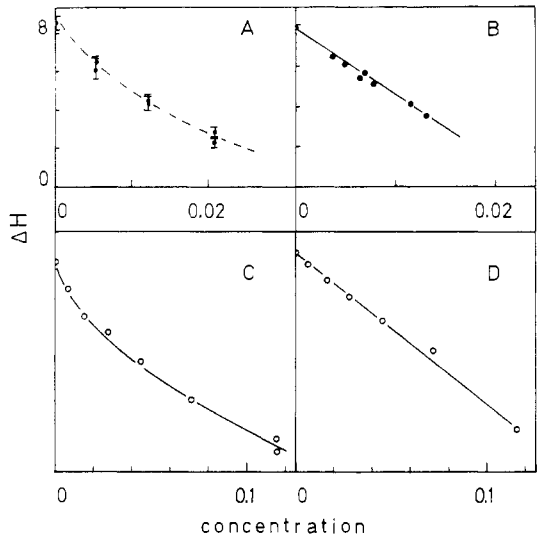

FIGURE 6: Transition enthalpy as a function of protein concentration calculated or measured as the area under the specific heat curve for DPPC–protein bilayers: (A) DPPC + lipophilin (Boggs et al., 1980); (B) DPPC + (Ca^{2+} + Mg^{2+})-ATPase from sarcoplasmic reticulum (Gomez-Fernandez et al., 1980; reproduced by permission). The units are kilocalories per mole. Calculated transition enthalpy for a DPPC bilayer with an integral protein of $M_r \simeq 15\,000$ and $K(G) = 0.204$: (C) Area under the specific heat curve calculated only under its peak at the upper phase boundary of the phase diagram (Figure 5). The c dependence is similar to that of Boggs et al. (1980). (D) Area under the specific heat peak calculated over a temperature range extending from the F phase to below T_K (Figure 4), similar to the linear plot of Gomez-Fernandez et al. (1980). Units here are arbitrary.

the temperature $T_K \approx 32$ °C, at which the protein cluster starts to melt. As the temperature is increased above T_K, the intensity decreases very quickly in a curve that may appear to depend linearly upon T. In fact, the shape of the curve between T_K and the temperature at which the intensity goes to zero reflects the upper phase boundary of Figure 4. One can thus get information about the phase boundaries directly from a measurement of the temperature and concentration dependence of this reflection. Figure 5 should be compared to Figure 5 of Hoffmann et al. (1980), who measured this reflection for the case of Ca^{2+}-ATPase from sarcoplasmic reticulum reconstituted in DPPC vesicles, and the results of our model support interpretation. It is clear from Figure 3 that the lipids which are melting in the reduction of the 4.2-Å reflection intensity are not those "trapped" inside the protein cluster but are those on the periphery of the cluster. It is thus not an "annulus" of lipids around a protein which is melting at T_K, because such an annulus, even if it existed, would be melted and statically disordered at $T = T_K$.

The question which thus arises is at what temperature and how do the lipids trapped between the proteins freeze into their G states. We have found that in models similar to those described here (Pink et al., unpublished results), they display noncooperative freezing over a temperature range of tens of degrees at ~−10 to −20 °C. This temperature will not necessarily be the same for *all* integral proteins.

In Figure 6, we have plotted the heat of transition as a function of protein concentration c, defined as the area under the specific heat curve, and the general shapes are compared to the measurements of Boggs et al. (1980) and Gomez-Fernandez et al. (1980). The shape, as a function of c, depends upon how the area is calculated. If only the area under the main lipid melting at ~40 °C is calculated, then a curve similar to that of Boggs et al. (1980) is obtained. If, however, the entire melting process from $T_K \approx 32$ °C and up is taken into account, a straight-line dependence similar to that obtained by Gomez-Fernandez et al. (1980) is found.

From the phase diagram, we can make some predictions about what should be observed with ^2H NMR. Experiments (Seelig & Seelig, 1978; Oldfield et al., 1978; Jacobs & Oldfield, 1981) show that in the fluid phase only one ^2H quadrupole powder-pattern splitting is seen, indicating a rapid exchange of lipids on a time scale of $\sim 10^{-5}$ s. That the splitting either is the same or is slightly less than that of pure lipids at the same temperature tells us approximately what the protein–lipid interaction, $K(G)$, is. As the system is cooled below T_c, phase separation starts to set in. Just below T_c, there will be lipid chains fluctuating rapidly between the G and e states together with some chains in the neighborhood of the proteins, being only in their e states. A fluid lipid powder-pattern should be seen together with a line shape characteristic of lipids undergoing fluctuations on a time scale slower than $\sim 10^{-6}$ s, this being the characteristic time for transitions of a free chain between the G and e states. As the temperature is lowered further, the fluctuating lipids become more frozen, their G $\rightleftarrows$ e fluctuations are very much reduced, and the ^2H NMR spectrum should approach a pattern characteristic of gel-phase lipids on which is superimposed a powder pattern characteristic of statically disordered chains. In some temperature range when T lies between T_c and $T_1 < T_c$, however, this description might be complicated by the rate of exchange of lipid molecules between the pure lipid phase and the protein-rich phase, so that one might not observe a gel phase pattern until T falls below T_1. Our model is unable as yet to suggest a value for T_1. Bearing in mind that when the lipid lateral diffusion coefficient is $D = 10^{-9}$ cm^2/s, then in 10^{-5} s, a lipid molecule will move a distance of ~10 Å, we see that T_1 may lie close to T_c. Another factor which will affect the ^2H NMR line shape is rotational diffusion, and this will probably not be frozen out until T is significantly below T_c (Davis, 1979). Our model does not consider lipid molecule rotation. If T_K lies sufficiently below T_c, then for $T < T_K$, a superposition of a gel-phase pattern and a small amount (depending upon the protein:lipid ratio in the protein-rich phase) of fluid lipid powder pattern will be seen.

Finally, we changed the protein–lipid interaction, $K(G)$, in order to see what effect this would have upon the quantities calculated above and the phase diagram. We chose $K(G) = 0.4$ instead of the previously used value of 0.204 which gives results for ^2H NMR static order parameters in accord with those measured (Kang et al., 1979; Pink et al., 1981a). The protein will now tend to statically order lipids adjacent to it much more than previously, and this should be reflected in the phase diagram.

Figure 7 shows the instantaneous values of $n_{pp}(T)$ as well as the average values $\overline{n_{pp}(T)}$ for various temperatures under the condition of slow cooling described before and is the counterpart of Figure 2. We see that there are still three regions on these graphs: the fluidlike region with a "random"-appearing distribution of protein, a region in which $\overline{n_{pp}(T)}$ rises as the proteins start to cluster, both of these regions exhibiting protein cluster fluctuations in $n_{pp}(T)$, and a third region where the fluctuations have been frozen out by the freezing of the lipids. By comparing these results to those of Figure 2, we see that although in both cases the values of $\overline{n_{pp}(T)}$ in the fluid region are the same the values of $\overline{n_{pp}(T)}$ in the region where "clustering" has been completed (at $T_K \approx 36$ °C) are significantly lower for $K(G) = 0.4$ than for the previous case. This is because the proteins now like to be adjacent to statically ordered chains much more than for the

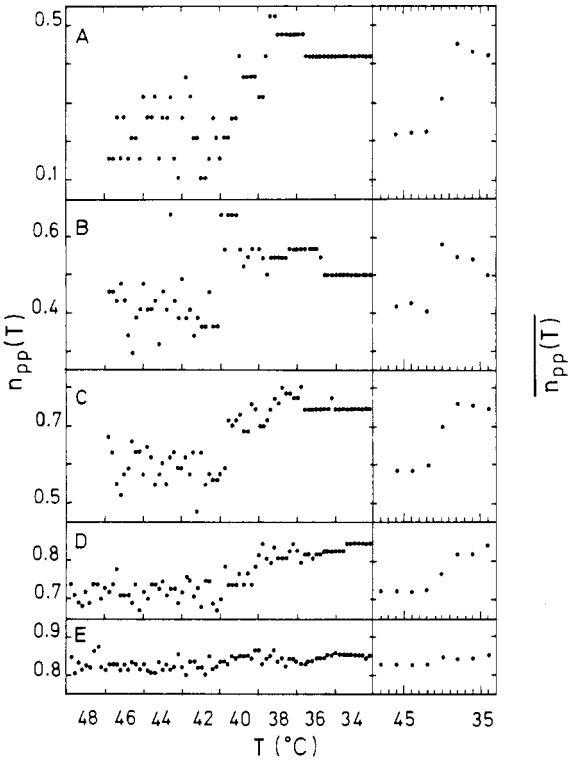

FIGURE 7: Number of protein–protein nearest neighbors, $n_{pp}(T)$ (left panels) and $\overline{n_{pp}(T)}$ (right panels), for $K(G) = 0.4$ and various protein concentrations, under conditions of slow cooling in a DPPC bilayer (see text). For $n_{pp}(T)$, each point represents its instantaneous value every 25 Monte Carlo steps, with the temperature being reduced by 2 °C every 250 steps. The system was first brought to equilibrium at 46 or 48 °C before being cooled. For $\overline{n_{pp}(T)}$, the points represent the average value of $n_{pp}(T)$ over 250 steps for each temperature. The number of proteins is the following: (A) 10; (B) 20; (C) 30; (D) 40; (E) 50. Fluctuations in $n_{pp}(T)$ indicate fluctuations in protein clustering.

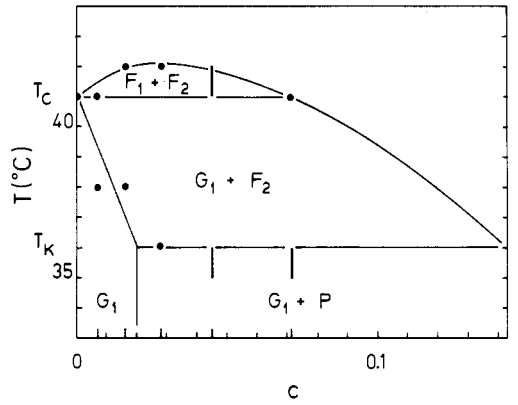

FIGURE 8: Approximate phase diagram for a DPPC–protein ($M_r \simeq 15000$) bilayer with $K(G) = 0.4$, deduced from Figure 7 as described in the text. F_1 and F_2 denote two fluid phases containing predominantly melted lipids. G_1 denotes a lipid-rich phase in which the lipid chains are predominantly in their extended conformations with a small amount of protein mixed in. P is a protein-rich phase. Markers along the c axis indicate the numbers of proteins from 10 to 50. $T_c = 41$ °C is the main pure DPPC melting temperature and $T_K \simeq 36$ °C, here, is the temperature at which the clusters in phase P start to come apart or melt. Vertical lines indicate uncertainties in the temperatures for various processes.

case $K(G) = 0.204$ and so mix better with lipids in the gellike phase than before. Thus, clustering will not be as pronounced (and indeed may appear to be absent in some cases) as it was for the case of $K(G) = 0.204$. If we plot the locus of the points denoting the onset of lipid chain freezing and those of the

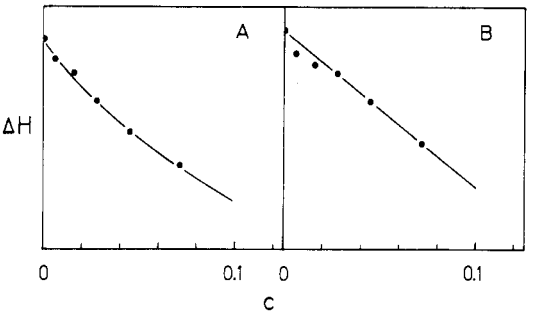

FIGURE 9: Calculated transition enthalpy (arbitrary units) for the DPPC–protein bilayer with $K(G) = 0.4$. (A) Area under the specific heat curve calculated only under its peak at the upper phase boundaries of the phase diagram (Figure 8). (B) Area under the specific heat peak calculated over a temperature range extending from the F_1 and F_2 phases to below T_K (Figure 8).

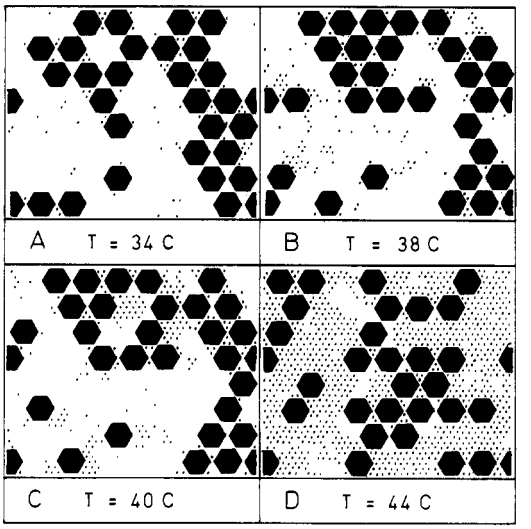

FIGURE 10: Typical protein distributions for $K(G) = 0.4$ at various temperatures for 30 proteins ($c = 0.028$). Black hexagons represent proteins, dots represent lipid chains in their e (melted) states, and blank area represent lipid chains in their G (extended) states. (A) Phase separation into lipid-rich and protein-rich phases, $G_1 + P$ (Figure 8), at $T = 34$ °C $< T_K$ ($\simeq 36$ °C here). (B and C) The protein-rich areas start to melt by melting lipid chains on their peripheries, and the proteins diffuse slightly apart at $T = 38$ °C and $T = 40$ °C. Note that the high value of $K(G)$ causes the proteins to keep the chains in their extended G states as shown by the large amount of G-state chains adjacent to proteins. (D) The lipid chains melt at $T \approx T_c$, and the protein distribution appears homogeneous in the plane of the bilayer as they diffuse more rapidly than at lower temperatures. The high value of $K(G)$ induces more chain ordering than before (compare Figure 3), and this will influence trans-bilayer diffusion (Zuckermann & Pink, 1980).

completion of the freezing out of fluctuations in $n_{pp}(T)$, then we obtain the phase diagram shown in Figure 8. We see that the stronger protein–lipid interactions, $K(G)$, have brought about the existence of a "low" concentration homogeneous lipid–protein phase (G_1) (which was not detected in the previous case but which probably exists at very low protein concentrations) as well as the possibility of two coexisting phases in the fluid region, F_1 and F_2. It should be realized, however, that these phase diagrams are only approximate, based as they are on changes in quantities which exhibit a good deal of fluctuations.

Figure 9 shows the transition enthalpy for this case, calculated either by considering only the enthalpy under the main melting specific heat peak at ~41 °C or by considering the transition to start at $T_K \approx 36$ °C. Again we find either a curve as reported by Boggs et al. (1980) or a straight line as reported

by Gomez-Fernandez et al. (1980). This difference is not a completely trivial point because it does depend on whether the coming apart of the protein-rich clusters is considered part of the main lipid melting or not.

Figure 10 shows the coming apart of the protein clusters for the case of 30 proteins with $K(G) = 0.4$ and should be compared to Figure 3. We see, as we expect, that the clusters are not as compact as in the previous case. At 34 °C, the clusters are just below their "melting" temperature of $T_K \approx$ 36 °C. At 38 and 40 °C, they are coming apart through a melting of the lipids on their peripheries, before the main lipid melting occurs at ~41 °C, while at 44 °C the entire system is melted.

It should be noted that even though the protein–lipid interaction, $K(G)$, has been increased by a factor of 2, the temperature T_K has been increased only by ~3 °C. We have taken this result together with other calculations using a mean field approximation (Pink et al., unpublished results) as a partial indication that T_K depends most strongly upon effective protein–protein interactions which are mediated by mechanisms other than through the lipid hydrocarbon chain interactions. Such interactions could arise, for example, through interaction with the water on either side of the bilayer. This will be studied elsewhere. The protein:lipid ratio in the protein-rich cluster will thus be determined not only by the protein–lipid interaction but also, and perhaps dominantly, by the effective protein–protein interaction.

Summary and Conclusions

We have studied an extension of a computer simulation model of a DPPC bilayer which contains integral proteins spanning the bilayer. This model allows the lipid hydrocarbon chains to be in either their "extended" state, G, or their "melted" state, e, and so they undergo a gel to liquid-crystal transition at a temperature $T_c = 41$ °C. The integral proteins can be as large as we wish and can undergo translational motion by moving between protein "cells". In the case studied here, the protein molecular weight was ~15000. We obtained the protein–lipid interaction energies, $K(n)$, by making use elsewhere of a mean field analysis of ^2H NMR measurements carried out at $T > T_c$. These results yielded $K(e) \simeq 0$ and $K(G) = 0.204$. We ignored both lipid molecule and protein rotational motion. In our simulation, there are two coupled dynamical processes taking place: (a) lipid chains attaining and maintaining a dynamic equilibrium in the G and e states and (b) protein molecules diffusing so as to approach equilibrium via lateral phase separation into random distributions or clusters exhibiting various degrees of compactness or ramification. These protein distributions are also dynamical fluctuating entities.

We observed the formation of protein-rich clusters and regions of nearly pure lipids as the system was cooled slowly to temperatures below T_c. Slow cooling is essential in order to allow proteins time to come to equilibrium at a given temperature. The phase diagram deduced for $K(G) = 0.204$ showed the following three regions: (i) A two-phase distribution composed of a protein-rich cluster and an essentially pure lipid phase for $T < T_K$ ($\simeq$32 °C here) was one region. The protein-rich region contained a minimum number of lipids, all of which remained in their melted state, e, on the average, down to 24 °C. (ii) For $T_K < T \lesssim T_c$, an essentially pure lipid phase coexists with the protein-rich cluster which gradually comes apart, thereby melting, as T increases. The cluster comes apart by incorporating more lipids into this phase. This is done by melting lipids on the periphery of the cluster which allows the proteins to diffuse apart. (iii) The lipid melting rate increases rapidly at some temperature between T_K and T_c (e.g., in the case of a lipid:protein ratio of 61:1, this occurs at $\simeq$40 °C) when the remainder of the lipids melt. For $T > T_c$, all the lipids are melted, on the average, and the proteins diffuse most rapidly and over some time interval display a random distribution.

By identification of the intensity of the 4.2 Å wide-angle X-ray reflection with the amount of pure lipid phase, the calculation of this intensity by using our phase diagram showed that the data of Hoffmann et al. (1980) could be completely understood. The temperature dependence of this intensity can give information directly about the shape of phase boundaries. Our model confirmed their interpretation and shows (Figure 3) the probable mechanism by which the protein-rich clusters melt by coming apart: The lipids on the periphery of the cluster melt which allows the proteins to diffuse apart. The lipids "trapped" between the proteins in the most compact clusters are all on the average melted at, and for some temperatures below, T_K and make essentially no contribution to transition enthalpies.

The dependence of the heat of transition, ΔQ, upon protein concentration, c, was shown to behave as already found experimentally, either to be linear or to be slightly concave as a function of increasing c, depending upon the temperature range considered to encompass the melting of the chains in the lipid bilayer. The calculated phase diagram showed that the behavior of ΔQ vs. c will not be like that displayed by bilayers which contain cholesterol instead of integral proteins.

We also studied the case of a strong protein–lipid interaction with $K(G) = 0.400$. The phase diagram is more complicated than that for $K(G) = 0.204$, displaying protein-rich, P, and lipid-rich, G_1, (but not pure lipid) phases down to 28 °C, as well as possibly a small two-phase region ($F_1 + F_2$) in the fluid phase for $T > T_c$ and another two-phase region $G_1 + F_2$ (Figure 8). Too much significance should not be attached to the possible existence of phases F_1 and F_2 over the 1 °C range shown in Figure 8. If they do exist, then F_1 is a lipid-rich phase with fluid lipids and F_2 contains a larger concentration of proteins than F_1 and may have lipid chains exhibiting more static order than those in F_1. The dependence of ΔQ upon c was essentially the same as that above, and a temperature T_K ($\simeq$36 °C) existed above which the protein-rich clusters started to come apart. The clusters were, however, not as compact as in the previous case, which was to be expected.

Acknowledgments

We are pleased to thank Dennis Chapman and Alex Georgallas for discussions regarding aspects of this paper and Greta Chisholm for typing the manuscript.

References

Alexandrowicz, Z. (1971a) *J. Chem. Phys. 55*, 2765–2779.
Alexandrowicz, Z. (1971b) *J. Stat. Phys. 5*, 19–34.
Binder, K. (1979) in *Monte Carlo Methods in Statistical Physics* (Binder, K., Ed.) pp 1–45, Springer-Verlag, West Berlin.
Boggs, J. M., Clement, I. R., & Moscarello, M. A. (1980) *Biochim. Biophys. Acta 601*, 134–151.
Davis, J. H. (1979) *Biophys. J. 27*, 339–358.
Dill, K. A., & Flory, P. J. (1980) *Proc. Natl. Acad. Sci. U.S.A. 77*, 3115–3119.
Domb, C., & Stoll, E. (1977) *J. Phys. A: Math. Gen. 10*, 1141–1149.
Freire, E., & Snyder, B. (1982) *Biophys. J. 37*, 617–624.
Georgallas, A., & Pink, D. A. (1982) *J. Colloid Interface Sci. 89*, 107–116.

Gomez-Fernandez, J. C., Goni, F. M., Bach, D., Restall, C. J., & Chapman, D. (1980) *Biochim. Biophys. Acta 598*, 502–516.
Hoffmann, W., Sarzala, M. G., Gomez-Fernandez, J. C., Goni, F. M., Restall, C. J., Chapman, D., Heppeler, G., & Kreutz, W. (1980) *J. Mol. Biol. 141*, 119–132.
Jacobs, R., & Oldfield, E. (1981) *Prog. Nucl. Magn. Reson. Spectrosc. 14*, 113–136.
Kang, S. Y., Gutowsky, H. S., Hsung, J. C., Jacobs, R., King, T. E., Rice, D., & Oldfield, E. (1979) *Biochemistry 18*, 3257–3267.
Marsaglia, G. (1968) *Proc. Natl. Acad. Sci. U.S.A. 61*, 25–28.
Metropolis, N., Rosenbluth, A. W., Rosenbluth, M. N., Teller, A. H., & Teller, E. (1953) *J. Chem. Phys. 21*, 1087–1092.
Nichol, C. P., Davis, J. H., Weeks, G., & Bloom, M. (1980) *Biochemistry 19*, 451–457.
Oldfield, E., Gilmore, R., Glaser, M., Gutowsky, H. S., Hshung, J. C., Kang, S. Y., King, T. E., Meadows, M., & Rice, D. (1978) *Proc. Natl. Acad. Sci. U.S.A. 75*, 4657–4660.
Overath, P., & Thilo, L. (1978) *Int. Rev. Biochem. 19*, 1–44.
Pink, D. A., & Zuckermann, M. J. (1980) *FEBS Lett. 109*, 5–8.
Pink, D. A., Green, T. J., & Chapman, D. (1980) *Biochemistry 19*, 349–356.
Pink, D. A., Georgallas, A., & Chapman, D. (1981a) *Biochemistry 20*, 7152–7157.
Pink, D. A., Green, T. J., & Chapman, D. (1981b) *Biochemistry 20*, 6692–6698.
Pink, D. A., Lookman, T., MacDonald, A. L., Zuckermann, M. J., & Jan, N. (1982) *Biochim. Biophys. Acta 687*, 42–56.
Rice, D. M., Meadows, M. D., Scheinman, A. O., Goni, F. M., Gomez, J. C., Moscarello, M. A., Chapman, D., & Oldfield, E. (1979) *Biochemistry 18*, 5893–5903.
Seelig, A., & Seelig, J. (1978) *Hoppe-Seyler's Z. Physiol. Chem. 359*, 1747–1756.
Skolnick, J., & Helfand, E. (1980) *J. Chem. Phys. 72*, 5489–5500.
Smith, I. C. P., Butler, K. W., Tulloch, A. P., Davis, J. H., & Bloom, M. (1979) *FEBS Lett. 100*, 57–61.
Stoll, E., & Domb, C. (1979) *J. Phys. A: Math. Gen. 12*, 1843–1855.
Weber, T. A. (1978) *J. Chem. Phys. 69*, 2347–2354.
Zuckermann, M. J., & Pink, D. A. (1980) *J. Chem. Phys. 73*, 2919–2926.

Rhodopsin–Phospholipid Reconstitution by Dialysis Removal of Octyl Glucoside†

Marilyn L. Jackson and Burton J. Litman*

ABSTRACT: Recombinant membranes were prepared from phospholipid-free rhodopsin and egg phosphatidylcholine (PC) under a wide variety of conditions employing an octyl β-D-glucoside (OG) dialysis procedure. Two bands were consistently observed after sucrose density centrifugation of these recombinants. The major band, which was protein rich, had a molar phospholipid:protein ratio that was in the range of 30:1 to 50:1, even when the molar phospholipid:protein ratio of the solubilized solution prior to OG removal was as high as 300:1. Similar results were obtained when dioleoyl-PC, 1-palmitoyl-2-oleoyl-PC, disk lipids, or diphytanoyl-PC was used instead of egg PC. These results can be explained in terms of a lower stability of the OG–phospholipid micelles relative to the OG–phospholipid–rhodopsin micelles. Of the phospholipids that were used in the OG dialysis procedure, only saturated dimyristoyl-PC produced a protein-rich recombinant band with a phospholipid:protein ratio close to that of the initial solubilized solution. In contrast to the results obtained by using OG, when solubilized disks supplemented with egg PC were reconstituted from sodium cholate or dodecyltrimethylammonium bromide, the resulting recombinant membranes had initial and final phospholipid:protein ratios which were similar.

Reconstitution of biological membranes is a powerful method of studying protein-lipid interactions (Razin, 1972) as well as protein function (Racker, 1979). Often specific reconstitution conditions and/or techniques must be chosen to obtain a desired reconstitution product. The underlying processes which lead to the formation of specific reconstituted forms is not well understood. Detailed studies of the reconstitution process in a variety of systems is likely to result in the formulation of a general set of principles which would serve as a guide in the formulation of reconstitution experiments. Relatively few such studies have been carried out.

The properties of the nonionic detergent octyl β-D-glucoside (OG),[1] which include its being nondenaturing to proteins

† From the Department of Biochemistry, University of Virginia School of Medicine, Charlottesville, Virginia 22908. *Received April 8, 1982.* This research was supported by National Science Foundation Grant PCM-8012028 and National Institutes of Health Grant EY00548. M.L.J. received support from National Institutes of Health Predoctoral Training Grant GM07294. A preliminary account of this work was presented at the Biophysical Discussions, Airlie, VA, Oct 1981.

[1] Abbreviations: GLC, gas–liquid chromatography; OG, octyl β-D-glucoside; PE, phosphatidylethanolamine, PC, phosphatidylcholine; PS, phosphatidylserine; DMPC, dimyristoylphosphatidylcholine; DOPC, dioleoylphosphatidylcholine; POPC, 1-palmitoyl-2-oleoylphosphatidylcholine; Tris, tris(hydroxymethyl)aminomethane; Hepes, *N*-(2-hydroxyethyl)piperazine-*N*′-2-ethanesulfonic acid; cmc, critical micelle concentration; EDTA, ethylenediaminetetraacetic acid; DTAB, dodecyltrimethylammonium bromide; TLC, thin-layer chromatography.

0006-2960/82/0421-5601$01.25/0